ANTIOXIDANTS & REDOX SIGNALING
Volume 19, Number 7, 2013

DOI: 10.1089/ars.2012.4625

Discoveries

FORUM ORIGINAL RESEARCH COMMUNICATION

Glutathione Transport: A New Role for PfCRT in Chloroquine Resistance

Eva-Maria Patzewitz,[1,2,*] J. Enrique Salcedo-Sora,[3,*] Eleanor H. Wong,[1] Sonal Sethia,[1] Paul A. Stocks,[3] Spencer C. Maughan,[4] James A.H. Murray,[4] Sanjeev Krishna,[5] Patrick G. Bray,[3] Stephen A. Ward,[3] and Sylke Müller[1]

Abstract

Aims: Chloroquine (CQ) kills *Plasmodium falciparum* by binding heme, preventing its detoxification to hemozoin in the digestive vacuole (DV) of the parasite. CQ resistance (CQR) is associated with mutations in the DV membrane protein *P. falciparum* chloroquine resistance transporter (PfCRT), mediating the leakage of CQ from the DV. However, additional factors are thought to contribute to the resistance phenotype. This study tested the hypothesis that there is a link between glutathione (GSH) and CQR. ***Results:*** Using isogenic parasite lines carrying wild-type or mutant *pfcrt*, we reveal lower levels of GSH in the mutant lines and enhanced sensitivity to the GSH synthesis inhibitor L-buthionine sulfoximine, without any alteration in cytosolic *de novo* GSH synthesis. Incubation with *N*-acetylcysteine resulted in increased GSH levels in all parasites, but only reduced susceptibility to CQ in PfCRT mutant-expressing lines. In support of a heme destruction mechanism involving GSH in CQR parasites, we also found lower hemozoin levels and reduced CQ binding in the CQR PfCRT-mutant lines. We further demonstrate *via* expression in *Xenopus laevis* oocytes that the mutant alleles of Pfcrt in CQR parasites selectively transport GSH. ***Innovation:*** We propose a mechanism whereby mutant *pfcrt* allows enhanced transport of GSH into the parasite's DV. The elevated levels of GSH in the DV reduce the level of free heme available for CQ binding, which mediates the lower susceptibility to CQ in the PfCRT mutant parasites. ***Conclusion:*** PfCRT has a dual role in CQR, facilitating both efflux of harmful CQ from the DV and influx of beneficial GSH into the DV. *Antioxid. Redox Signal.* 19, 683–695.

Introduction

Until the widespread emergence of parasite resistance, the antimalarial chloroquine (CQ) was one of the most important drugs ever developed. Despite its clinical importance, the molecular basis of CQ resistance (CQR) is still not fully resolved. CQ action depends on binding to heme, a toxic byproduct of host hemoglobin degradation by the malaria parasite *Plasmodium falciparum*. This degradation occurs in the digestive vacuole (DV) of the intraerythrocytic parasite (8), with the heme generated not being destroyed enzymatically,

Innovation

We provide data that support a novel hypothesis for the role of mutant *Plasmodium falciparum* chloroquine resistance transporter (PfCRT) in the chloroquine resistance phenotype. The data indicate that mutant PfCRT facilitates the redistribution of glutathione (GSH) from the cytoplasm to the digestive vacuole. This results in GSH-dependent removal of heme-binding sites, both directly by occupying them and indirectly through causing heme breakdown, which is a significant contributor to the decrease in chloroquine susceptibility.

[1]Institute of Infection, Immunity and Inflammation, College of Medical, Veterinary and Life Sciences, University of Glasgow, Glasgow, United Kingdom.
[2]Faculty of Medical and Health Sciences, University of Nottingham, Nottingham, United Kingdom.
[3]Molecular and Biochemical Parasitology Group, Liverpool School of Tropical Medicine, Liverpool, United Kingdom.
[4]School of Biosciences, Cardiff University, Cardiff, United Kingdom.
[5]Cellular and Molecular Medicine, St. George's, University of London, London, United Kingdom.
*These authors have contributed equally.

but instead being converted into a relatively inert biocrystal called hemozoin (34). The binding of CQ to heme inhibits hemozoin formation, thus resulting in a build-up of free heme and CQ–heme complexes, which results in inhibition of parasite growth and eventually parasite death (44).

CQR correlates with reduced accumulation of drug in the parasite due to diminished drug–heme binding in the DV, although other interpretations have been recently suggested (5, 7). CQR is associated with polymorphisms within the DV transmembrane protein PfCRT (11, 17, 18, 42). A K76T mutation in PfCRT is conserved in all CQR parasites and is considered key in mediating the CQR phenotype (18). However, there is a wide variation in the response to CQ of cloned parasite lines containing identical mutant *pfcrt* alleles, which indicates the involvement of additional mechanisms contributing to CQR. The multidrug-resistant homolog gene *pfmdr1* is probably one (12, 32, 37), but it is likely that other factors also modify susceptibility to CQ.

Research reported during the last three decades has pointed to glutathione (GSH), the major antioxidant thiol in the parasite (2), playing some part in CQR (1, 13, 14). One possible mechanism would be that GSH reduces heme-binding sites for CQ in some way. We postulated that different concentrations of membrane-impermeant GSH in the DV of CQR and chloroquine-sensitive (CQS) parasites could be the basis of such a mechanism. To investigate this, GSH concentrations have been compared between the CQS and CQR lines. The data generated, however, have been difficult to interpret, as isolates with different genetic backgrounds were used (30). It is thought that such lines have variable transcriptional and translational regulation of oxidative defenses and efflux transporters such as PfMRP1, which affects GSH levels (23, 31, 36). Thus, we have now analyzed in this study isogenic parasite lines, which differ only in their substituted *pfcrt* allele (Table 1) (42). We have confirmed that GSH is generated in the cytoplasm and demonstrate that artificially increasing GSH levels has little effect on CQ sensitivity unless the parasites also harbor mutant alleles of *pfcrt*. Moreover, we show that mutant PfCRT can transport GSH. This newly discovered function facilitates GSH redistribution from the cytoplasm into the DV selectively in the CQR lines. The data generated have allowed us to postulate a CQ resistance mechanism in which GSH is selectively transferred into the DV *via* mutant *pfcrt*, where it competes with CQ for heme binding and results in destruction of heme, and thereby protects the parasites from the prooxidant activity of the CQ–heme complex.

Table 1. Genotypes and Phenotypes of Parasites Used in This Study

Parasite line	*Genetic modification*	*Susceptibility to CQ*
GC03	NONE	Sensitive
Dd2	NONE	Resistant
$C2^{GC03}$	*crt* locus of GC03 replaced by GC03 *crt* locus (42)	Sensitive
$C3^{Dd2}$	*crt* locus of GC03 replaced by Dd2 *crt* locus (42)	Resistant
$C6^{7G8}$	*crt* locus of GC03 replaced by 7G8 *crt* locus (42)	Resistant
T76K-1^{Dd2}	*crt* locus of Dd2 replaced by Dd2 *crt* locus T to K back mutant (9)	Sensitive
C-1^{Dd2}	*crt* locus of Dd2 replaced by Dd2 *crt* locus (18)	Resistant

CQ, chloroquine.

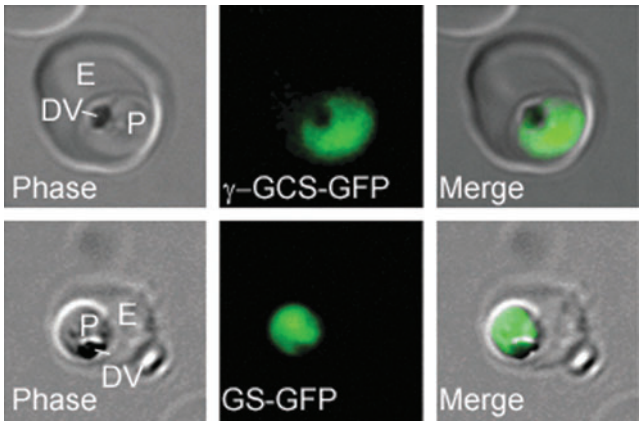

FIG. 1. Localization of *Plasmodium falciparum* γ-glutamylcysteine synthetase–green fluorescent protein (PfγGCS-GFP) and glutathione synthetase-GFP (PfGS-GFP). *P. falciparum* GS and γGCS C-terminally tagged with GFP were expressed in *P. falciparum* D10 erythrocytic stages. Fluorescence was analyzed using an Axioskop-2 mot plus microscope (Zeiss) equipped with a Hamamatsu C4742-95 CCD camera and was shown to be present throughout the cytoplasm of both transfected parasite lines, suggesting that GSH biosynthesis is cytoplasmic. No fluorescence is seen in the digestive vacuoles (DV) of the parasites or the erythrocyte host cell (E). E, erythrocyte; P, parasite; DV, digestive vacuole with hemozoin crystals.

Results

Localization of GSH biosynthesis enzymes

P. falciparum possesses genes encoding γ-glutamylcysteine synthetase (*PfγGCS*) and glutathione synthase (*PfGS*), required for GSH synthesis (24, 29). C-terminally tagged green fluorescent protein (GFP) variants of each gene were transfected into *P. falciparum*, and the resultant line expressed proteins were both localized to the parasite cytosol (Fig. 1).

GSH levels in isogenic lines and their susceptibility to GSH-depleting agents

Total GSH levels of isogenic parasite lines GC03, $C2^{GC03}$, $C3^{Dd2}$, and $C6^{7G8}$ (Table 1) were determined using a validated HPLC method (42, 51). Transfected parasites carrying the Dd2 or 7G8 *pfcrt* CQR alleles contained significantly less GSH than the lines carrying the sensitive HB3 wild-type *pfcrt* allele (Fig. 2A). We also determined the GSH levels of the nonisogenic untransformed CQR Dd2 standard laboratory parasite line (see Table 1) and found no significant difference in GSH content between this line and the isogenic CQS parasites whose genotype is that of GC03 (see Table 1) (Dd2, 984 ± 184 nmol/10^{10}cells; $C2^{GC03}$, 1152 ± 93 nmol/10^{10}cells). These data highlight the importance of our use of the isogenic parasite lines, because this allowed us to probe specifically the effect of mutations in *crt* on GSH levels and avoided the problems associated with the confounding effects of other compensatory changes that would be likely to have occurred in untransformed CQR isolates.

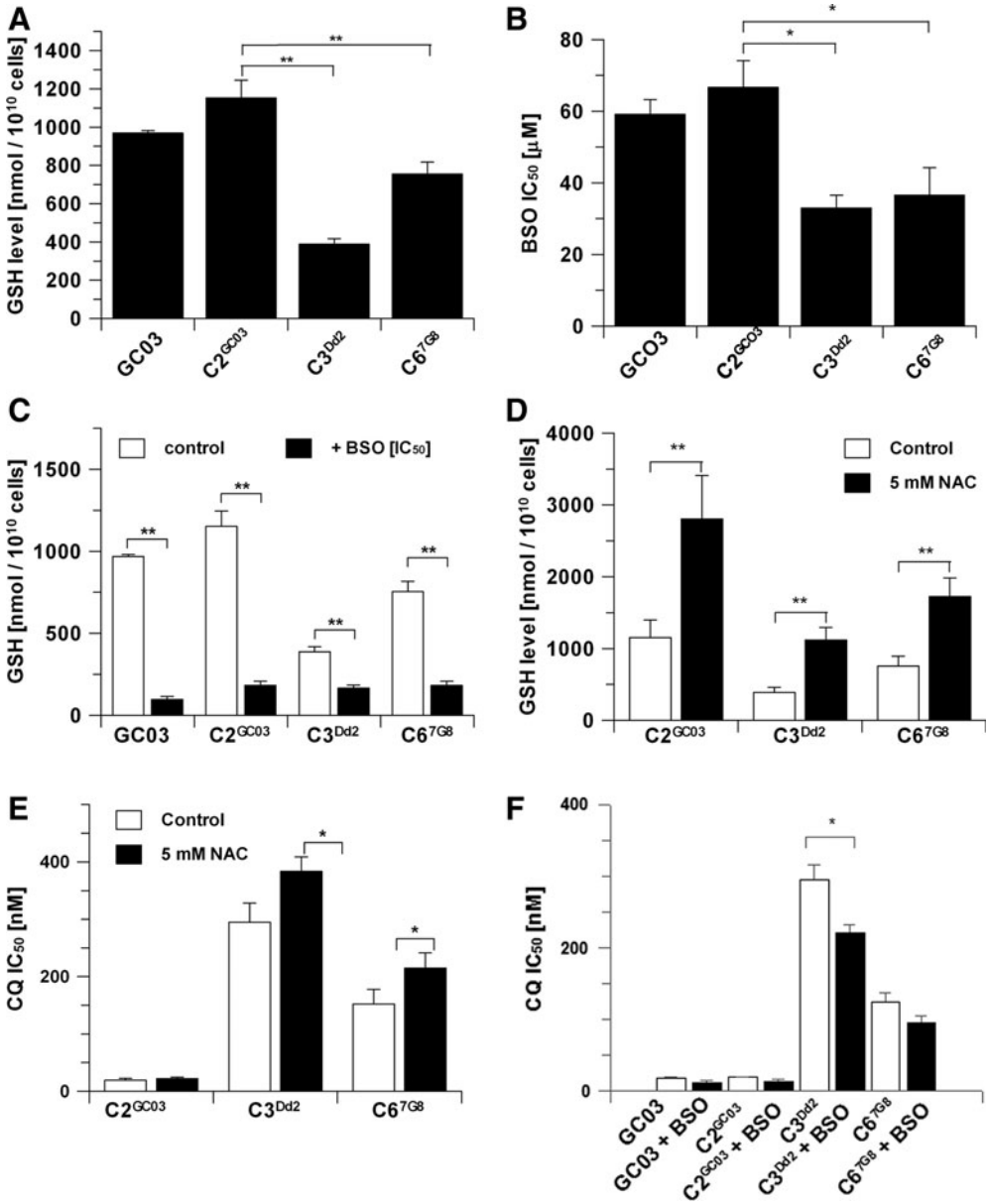

FIG. 2. Glutathione (GSH) levels, susceptibility to L-buthionine sulfoximine (BSO) and the effect of *N*-acetylcysteine (NAC) on chloroquine (CQ) susceptibility. (A) The GSH levels in $C3^{Dd2}$ (388 ± 29 nmol/10^{10} cells, $n = 6$) and $C6^{7G8}$ (754 ± 61 nmol/10^{10} cells, $n = 5$) were significantly lower than those determined in $C2^{GC03}$ (1152 ± 93 nmol/10^{10} cells, $n = 6$) and GC03 (968 ± 12 nmol/10^{10} cells, $n = 3$) (**$p < 0.01$, one-way analysis of variance (ANOVA) with Newman–Keuls post-test). Data represent means ± S.E.M. **(B)** IC_{50} values for BSO (48 h assay) for the CQR parasite lines $C3^{Dd2}$ (IC_{50}: 32.9 ± 3.5 μM) and $C6^{7G8}$ (IC_{50}: 36.5 ± 7.7 μM) were significantly lower than that of CQS $C2^{GC03}$ and GC03 (IC_{50}: 60.3 ± 8.3 μM and 59.1 ± 4.1 μM) (*$p < 0.05$, one-way ANOVA with Newman–Keuls post-test). Data represent means ± S.E.M. ($n = 9$). **(C)** Parasite lines were exposed to IC_{50} concentrations of BSO for 2 h before GSH levels were determined. GSH levels decreased significantly in all 4 parasite lines: from 968 ± 12 to 97 ± 17 nmol/10^{10} cells for GC03; from 1152 ± 93 to 183 ± 24 nmol/10^{10} cells for $C2^{GC03}$; from 388 ± 29 to 166 ± 19 nmol/10^{10} cells for $C3^{Dd2}$; and from 754 ± 61 to 183 ± 24 nmol/10^{10} cells for $C6^{7G8}$. Data represent means ± S.E.M. of two to six independent measurements (**$p < 0.01$, one-way ANOVA with Newman–Keuls post-test). **(D)** The levels of GSH in $C2^{GC03}$, $C3^{Dd2}$, and $C6^{7G8}$ were determined after incubation without or with 5 m*M* NAC for 16 h. The levels of the GSH increased significantly in all three parasite lines analyzed to from 1152 ± 93 to 2800 ± 600 nmol/10^{10} cells for $C2^{GC03}$; from 388 ± 29 nmol/10^{10} cells to 1120 ± 180 nmol/10^{10} cells for $C3^{Dd2}$; and from 754 ± 61 nmol/10^{10} cells to 1720 ± 260 nmol/10^{10} cells for $C6^{7G8}$. Data represent means ± S.E.M. of two independent experiments each done in triplicate (**$p < 0.01$; one-way ANOVA with Newman–Keuls post-test). **(E)** The effect of 5 m*M* NAC on the susceptibility to CQ was determined. In a normal medium, IC_{50}s were 19.2 ± 3.2 n*M*, 295 ± 33 n*M*, and 152 ± 25 n*M* for $C2^{GC03}$, $C3^{Dd2}$, and $C6^{7G8}$, respectively. In the presence of 5 mM NAC, the IC_{50}s increased significantly in $C3^{Dd2}$ to 384 ± 25 n*M* and in CQR $C6^{7G8}$ to 215 ± 27 n*M* (*$p < 0.05$; one-way ANOVA with Newman–Keuls post-test), while the IC_{50} for $C2^{GC03}$ (21.9 ± 3.0 n*M*) was not significantly different. Data represent means ± S.E.M. of three to four independent experiments each done in triplicate. **(F)** The effect of preincubating parasite lines with 30 μM BSO (CQR) or 60 μM BSO (CQS) on their susceptibility to CQ for 20 h was analyzed. The IC_{50} values decreased from 18.3 ± 0.9 n*M* to 11.5 ± 3.7 n*M* in GC03; 19.3 ± 1.2 n*M* to 13.0 ± 4.1 n*M* in $C2^{GC03}$; from 296 ± 21 n*M* to 222 ± 11 n*M* in $C3^{Dd2}$; and from 125 ± 12 n*M* to 93.3 ± 9.3 n*M* in $C6^{7G8}$. The reduction of the CQ IC_{50} in $C3^{Dd2}$ was significant (*$p < 0.05$; one-way ANOVA with Newman–Keuls post-test).

To elucidate whether the isogenic lines were differentially affected by the specific γGCS inhibitor L-buthionine sulfoximine (BSO), the IC_{50} values of BSO were determined (Fig. 2B). Consistent with the lower GSH levels in the CQR lines, the IC_{50} values for BSO of these parasites were approximately half those of the CQS lines (Fig. 2B). It was further verified that the lethal effect of BSO was associated with GSH depletion. BSO treatment at IC_{50} concentrations (for 2 h) resulted in significant decreases of GSH levels in all four parasite lines (Fig. 2C).

Susceptibility of parasite lines to CQ and the effect of N-acetylcysteine

Incubating the isogenic parasites with 5 mM *N*-acetylcysteine (NAC) for 16 h increased intracellular GSH levels in the CQS $C2^{GC03}$ line by more than twofold (Fig. 2D) without causing a significant change in the response to CQ, the IC_{50} ratio being 1.1 (Fig. 2E). In contrast, increasing GSH levels in the CQR parasites $C3^{Dd2}$and $C6^{7G8}$ (Fig. 2D) led to statistically significant increases of the CQ IC_{50} values of both lines (Fig. 2E). These data support the case that elevated GSH levels in the presence of the mutant *crt* gene mediate a further increase in the resistance to CQ. Additional supporting evidence for the involvement of GSH and CRT was provided by the demonstration that a decrease in GSH levels by preincubation of parasites with BSO resulted in a significant reduction in CQ IC_{50} in $C3^{Dd2}$ (Fig. 2F).

Effect of moderating intracellular GSH levels on CQ accumulation

The $C2^{GC03}$ and $C3^{Dd2}$ lines were treated with 1-chloro-2, 4-dinitrobenzene (CDNB), a substrate for glutathione *S*-transferase (GST) that leads to the formation of 2,4-dinitrophenyl-*S*-glutathione adducts, which are excreted, and thus result in a decrease of intracellular GSH levels (22, 28), and their effect on accumulation of CQ was measured. Increasing concentrations of CDNB to just above the IC_{50} concentrations ($8.5 \pm 4.5\ \mu M$ and $9.5 \pm 1.1\ \mu M$ for $C2^{GC03}$ and $C3^{Dd2}$, respectively) significantly stimulated the accumulation of [^{3}H]-CQ in the CQR parasite line $C3^{Dd2}$, but not in the CQS line $C2^{GC03}$ (Fig. 3A). The CDNB effect on [^{3}H]-CQ accumulation in CQR parasites was similar to that caused by 10 μM verapamil (VP) (Fig. 3A), which is an L-type calcium channel blocker known to interact with mutated forms of PfCRT (18, 26, 33, 42). In contrast, [^{3}H]-CQ accumulation in CQS $C2^{GC03}$ was unaffected by CDNB or VP (Fig. 3A). Qualitatively similar results were obtained comparing a CQS back-mutant parasite line derived from a CQR parent line (Dd2) called T76K-1^{Dd2} (Table 1) with the CQR C-1^{Dd2} (Table 1) (Fig. 3B) (18). The effect of 10 μM CDNB and VP was negligible in the CQS T76K-1^{Dd2}, whereas the effects on the CQR line C-1^{Dd2} were similar to that observed with $C3^{Dd2}$ (Fig. 3B). It was confirmed that incubation with 20 μM CDNB for 20 min (the same incubation time as in the cellular accumulation ratio for chloroquine experiment described above) resulted in significantly reduced GSH levels (Fig. 3C). These data show that the reduced GSH levels resulting from CDNB treatment impact on CQ accumulation, but only in parasites carrying the K76T mutation in the *pfcrt* allele. An alternative explanation could be that the 2,4-dinitrophenyl-*S*-glutathione adduct generated itself interferes with CQ movement through mutant PfCRT in a similar way to VP.

CQ equilibrium binding studies and the concentration of hemozoin

The data detailed above suggested that cytoplasmic GSH may have access to the DV in CQR parasites and thus be able to interact with the free heme there to form a GSH–heme complex, possibly with the neutral thiol serving as an axial ligand to heme iron as suggested by Shviro and Shaklai (41). This interaction would scavenge free heme and slow down the rate of hemozoin formation, but as the GSH–heme complex is nontoxic (41), it would not damage the parasite, and would also compete with CQ for binding to the heme target and so reduce the toxicity of CQ. In addition, it is possible that some of the heme could be spontaneously destroyed by GSH, liberating iron and GSSG (1, 41), which would also result in reducing CQ binding and so its antimalarial effectiveness.

For these reasons, we postulated that the amount of free heme in the DV of CQR parasite lines should be reduced. It is difficult to measure directly the concentration of free heme in the DV of *P. falciparum*, but its concentration can be reliably estimated from analysis of the CQ equilibrium binding experiments performed on intact infected erythrocytes (4, 5, 9). The basis of this assay is that CQ readily forms a complex with free heme and so prevents its biomineralization into hemozoin (3, 5). Our analysis of the apparent affinity of CQ binding to heme demonstrated that it is greatly reduced in the CQR lines $C3^{Dd2}$ and $C6^{7G8}$ compared to the $C2^{GC03}$ CQS line (Fig. 3D), with both reduced apparent affinity and also reduced heme-binding capacity. Least-squares analysis of the CQ-binding isotherms indicates that CQ equilibrium binding capacity is lower in $C3^{Dd2}$ and $C6^{7G8}$ isolates ($30 \pm 0.8\ \mu M$ and $29 \pm 1.7\ \mu M$, respectively) compared to $C2^{GC03}$ ($35 \pm 1.1\ \mu M$). This is consistent with free heme availability being less, although only by about 15%, in these two CQR lines and potentially linked to mutations in PfCRT. The decreases are also consistent with the 15%–20% reduction in CQ-binding capacity reported in the CQR progeny of a genetic cross [reported as J_{max} in Sanchez *et al.* (40)].

We also determined hemozoin levels in the CQS and CQR lines, and showed that they were significantly lower ($p < 0.001$) in CQR $C3^{Dd2}$ compared with CQS $C2^{GCO3}$ (Fig. 3E). Consistent with the model, we propose that GSH in CQR parasites scavenges or destroys free heme. It should be noted that a report by Gligorijevic and colleagues (15) concluded that there was no difference in the hemozoin content between untransformed GC03 and transformed $C3^{Dd2}$. In that study, hemozoin quantity was determined indirectly from the volume of the malaria pigment as measured microscopically, whereas we used a quantitative chemical assay. This may suggest that pigment volume and hemozoin content are not linearly correlated.

Expression of GSH biosynthesis and GSH-dependent enzymes

To investigate whether the lower levels of GSH observed in the untreated lines with the mutant CRT could result from differential expression of GSH biosynthetic genes, real-time quantitative polymerase chain reaction (RT-PCR) of *pfgs* and *pfγgcs* was undertaken. This revealed only slight variations in the expression of these genes between parasite lines (Fig. 4A), ruling out that the different GSH levels were a consequence of reduced GSH biosynthesis in the CQR parasites. Moreover, the levels of expression of *pfcrt* mRNA were equivalent in the four

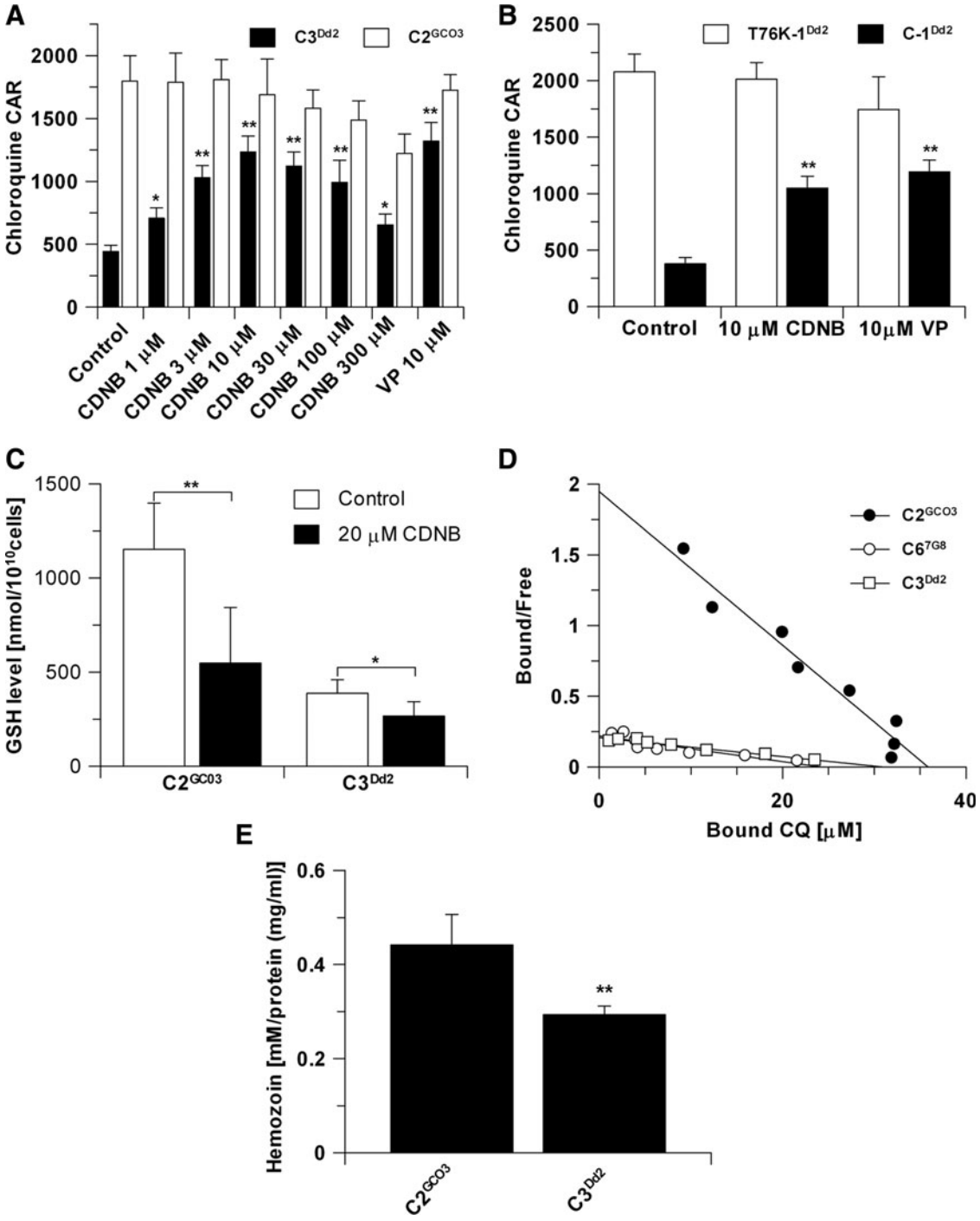

FIG. 3. Differential effect of 1-chloro-2,4-dinitrobenzene (CDNB) on CQ accumulation and differences in CQ binding between CQ-sensitive (CQS) and CQ-resistant (CQR) lines. (A) The effect of a range of concentrations of CDNB on the steady-state cellular accumulation ratio (CAR) of [^{3}H]-CQ in the C2^{GC03} CQS line (open bars) and the C3^{Dd2} CQR line (filled bars). Significant differences to the control are indicated by *($p < 0.05$) and **($p < 0.01$). Statistical analysis was performed using one-way ANOVA with Newman–Keuls post-test. The effect of 10 μM CDNB is comparable to that of 10 μM verapamil (VP). **(B)** The effect of 10 μM CDNB on CAR of [^{3}H]-CQ in the T76K-1^{Dd2} back-mutant CQS line (open bars) and the C-1^{Dd2} CQR line (filled bars) and the comparative effect of 10 μM VP (**$p < 0.01$). **(C)** Effect of 20 μM CDNB on the levels of GSH in the isogenic parasite lines differing in their PfCRT allele. The parasites were incubated for 20 min before GSH levels were determined (*$p < 0.05$). **(D)** Scatchard plot of CQ equilibrium binding in the C2^{GC03} CQS line (filled circles), the C3^{Dd2} CQR line (open squares), and the C6^{7G8} CQR line (open circles). Data are means of single observations derived from five individual experiments. **(E)** Normalized hemozoin content of the C2^{GC03} CQS and C3^{Dd2} CQR lines. Data represent means ± S.D. of 10 individual preparations of hemozoin normalized to parasite protein concentration (**$p < 0.01$; one-way ANOVA with Newman–Keuls post-test).

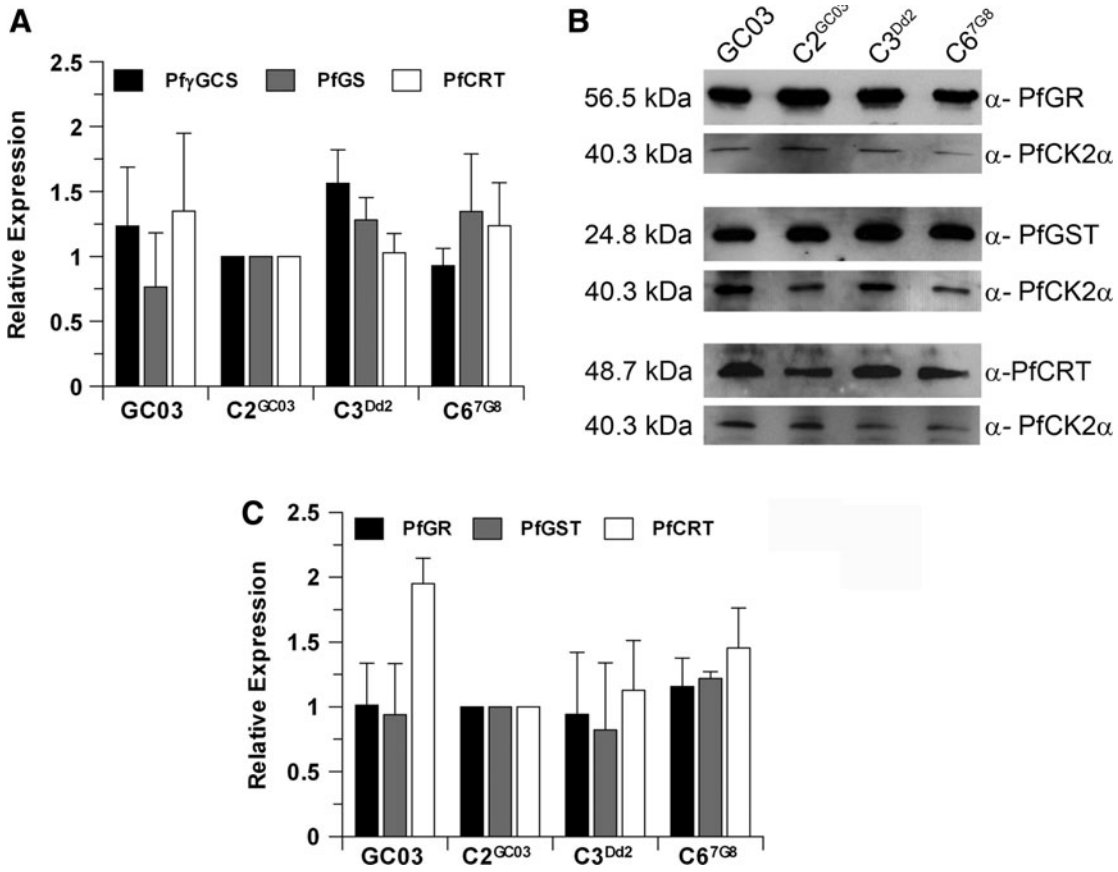

FIG. 4. Expression level of GSH biosynthesis genes, GSH-dependent proteins, and *Plasmodium falciparum* chloroquine resistance transporter (PfCRT). (A) The expression levels of *γgcs*, *gs*, and *pfcrt* in GC03, $C3^{Dd2}$, and $C6^{7G8}$ were analyzed by real-time quantitative PCR relative to the expression levels of $C2^{GC03}$ as outlined in the Materials and Methods section. The expression was normalized using the *seryl-t-RNA* message, which is uniformly expressed throughout the parasite blood-stage cycle. The data shown are means ± S.E.M. of three independent experiments, each performed in triplicate. **(B)** Western blots of saponin-isolated parasite lysates of CQS and CQR parasite lines were performed with 5 μg of protein per lane. The blots were probed with rabbit anti-PfGR antibodies (1:15,000) (α-PfGR) or rabbit anti-PfGST (1:5,000) (α-PfGST) to assess the level of each protein in the different parasite lines. The blots were reprobed with rabbit anti-PfCK2a (α-PfCK2a) diluted 1:200 to control for equal loading. **(C)** The relative expression of proteins shown in B was analyzed using LabImage 1D, and the data represent the normalized mean values obtained from three to four independent western blots ± S.D. Protein expression levels showed no significant differences.

parasite lines. In addition, PfCRT protein expression, as determined by western blotting, was similar in the three isogenic lines $C2^{GC03}$, $C3^{Dd2}$, and $C6^{7G8}$, while the parent line GC03 contained 1.5-fold to 2-fold higher levels of PfCRT protein (Fig. 4B, C), which is consistent with previous reports by Sidhu and colleagues (42). The levels of *P. falciparum* glutathione-*S*-transferase (*Pf*GST) and *P. falciparum* glutathione reductase (PfGR) proteins were similar in all parasite lines (Fig. 4B, C), suggesting that the CQR parasites preserve their capacity to maintain their redox status through the action of PfGR and to generate conjugates with GSH through the activity of PfGST. One caveat is that we cannot exclude the possibility that PfGST activity might be negatively affected by the lower GSH levels in the CQR parasite lines.

GSH transport activity of PfCRT expressed in Xenopus oocytes

The data above demonstrate that the presence of mutant *pfcrt* leads to a reduction in intracellular GSH levels in CQR parasites without any alterations in GSH metabolism. Further, the mutant allele is required to demonstrate an effect of CDNB on CQ accumulation and to show an increase in CQ IC_{50} values in the presence of NAC. We thus hypothesized that these effects are mediated by selective transfer of GSH to the DV, the site of CQ action, possibly *via* transport by mutant PfCRT that is located in the DV membrane (49). This hypothesis was tested using the *X. laevis* heterologous expression system to express mutant and wild-type forms of PfCRT. This system has been previously validated experimentally as being suitable for measurement of GSH uptake in a study of a family of PfCRT-like proteins occurring in *Arabidopsis thaliana* (AtCLT), which are GSH transporters (27). Further evidence for the suitability of the assay system was provided by measuring the uptake of [^{3}H]-CQ into oocytes expressing the $PfCRT^{Dd2}$ variant (26).

We expressed several PfCRT variants in *Xenopus* oocytes: $PfCRT^{HB3}$ as a representative of the CQS wild-type allele of *pfcrt*, as carried by $C2^{GC03}$; $PfCRT^{Dd2}$ as the predominant CQR mutant from Southeast Asia and the PfCRT isoform found in

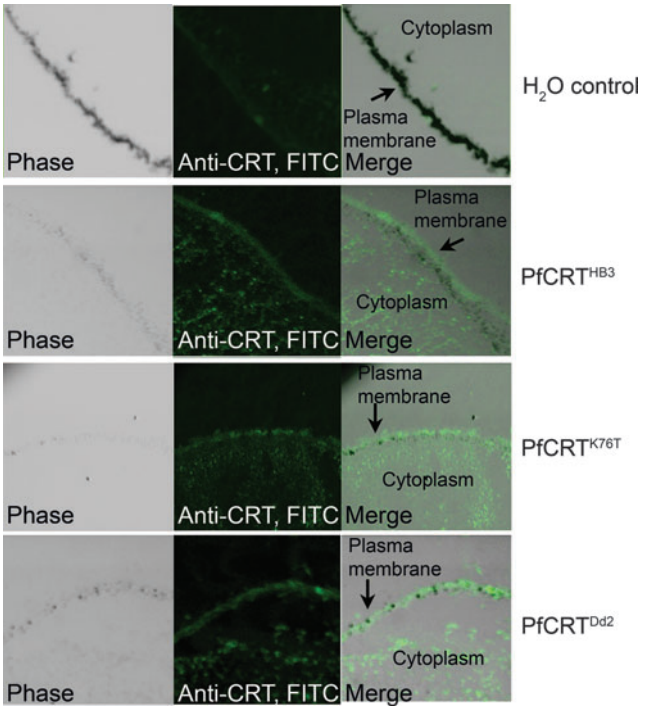

FIG. 5. Functional expression of PfCRT in *Xenopus* oocytes. Indirect immunofluorescence images of individual *X. laevis* oocytes after sectioning, fixing, and probing with the primary anti-PfCRT (1:500) (11) and the secondary anti-rabbit (1:500) IgG antibodies. Images shown are phase contrast (left panel), secondary antibody fluorescence (center panel), and merged (right panel). Images are presented for water-injected control oocytes and oocytes expressing the HB3, K76T, and Dd2 variants of PfCRT (top to bottom). The plasma membrane and cytoplasm are labeled.

$C3^{Dd2}$; $PfCRT^{K76T}$ as it carries only the single K76T mutation, but is otherwise wild type (a form that has no corollary in parasite isolate lines); *A. thaliana* CLT1 (AtCLT1) as a positive control. Indirect immunofluorescence was performed using anti-PfCRT as the primary antibody (11). The images demonstrated that $PfCRT^{HB3}$, $PfCRT^{K76T}$, and $PfCRT^{Dd2}$ were all expressed in the oocytes injected with the cRNA of their respective genes (Fig. 5). Immunofluorescence is visible at the plasma membrane and also in the cytoplasm at comparable levels for all three PfCRT variants. There is no fluorescence signal in the water-injected control group.

We confirmed previous reports that oocytes expressing $PfCRT^{Dd2}$ demonstrated a two-threefold increase in [^{3}H]-CQ uptake compared to water-injected controls, an effect that was time dependent (Fig. 6A) (26). The *X. laevis* oocytes possess a low endogenous ability to take up GSH, which has been observed in previous studies (21, 27). The expression of $PfCRT^{Dd2}$, however, conferred time-dependent transport of [^{3}H]-GSH, which was reduced to basal levels in the presence of CQ (Fig. 6B). $PfCRT^{Dd2}$ and $PfCRT^{K76T}$ showed six- and twofold higher rates of GSH membrane transport than water-injected controls. [^{3}H]-GSH uptake into oocytes expressing $PfCRT^{Dd2}$ or $PfCRT^{K76T}$ was specific, with transport inhibited by saturating concentrations of unlabeled GSH, CQ, and VP (Fig. 6D). No transport of [^{3}H]-GSH was detected in oocytes expressing $PfCRT^{HB3}$, showing that only the CQR isoforms of PfCRT transport GSH (Fig. 6C). Thus, these findings strongly support the proposal that the mutant PfCRT occurring in CQR parasites transport GSH.

Discussion

It is widely acknowledged that resistance to CQ is primarily conferred by mutations in the *P. falciparum* transporter gene *pfcrt* (11, 17, 42, 49), although other factors, including the multidrug-resistant transporter homolog *pfmdr1*, also contribute to the level of CQR (32, 37). This current study re-evaluated the hypothesis that GSH plays a part in CQR (14) and has revealed a previously unconsidered role for the CQR alleles of *pfcrt*. GSH was reported previously to scavenge free heme, forming a complex in which the thiol group is linked to heme iron, and provides a mechanism to protect membranes from oxidative heme damage (41). CQ also binds to heme, inhibiting the detoxification of heme into hemozoin crystals and causing a build-up of a drug–heme complex (4, 9, 18, 20, 50). This CQ–heme complex is toxic, in contrast to the GSH–heme complex, promoting lipid peroxidation and destruction of parasite membranes and mediates parasite killing by CQ (41). Thus, it can be envisaged that GSH could interfere with CQ action simply by competing for binding with heme. It has also been reported that GSH degrades heme *in vitro* (1, 41); if this happens *in situ*, then GSH would interfere with CQ action by destroying its target. A third possibility whereby GSH could play a role is that it may protect parasites from enhanced heme-induced oxidative stress (2). Our data showing that CQR *P. falciparum* contains reduced levels of hemozoin are consistent with free heme being either scavenged or degraded by GSH in these parasites. However, until now, it was not clear how modulating the levels of GSH, which is synthesized in the cytoplasm of the parasites, can influence the sensitivity to CQ, which acts within the DV of the parasites where heme is generated.

Our findings in this study resolve this issue and reveal a new role for mutant PfCRT in transporting GSH between the cytoplasm and the DV, presumably leading to a change in the overall distribution of the tripeptide. We demonstrate direct and specific transport of GSH by two CQR isoforms (K76T and Dd2) of PfCRT expressed in *X. laevis* oocytes. Further evidence for mutant PfCRT-driven GSH transport is provided by selective inhibition of GSH uptake by both CQ and VP. GSH transport by CQR alleles of *pfcrt* is in agreement with a previous report that the CQR mutant $PfCRT^{Dd2}$ is capable of transporting small peptides as well as CQ (26). In fact, we found that a single-point mutant $PfCRT^{K76T}$ was sufficient to allow uptake of [^{3}H]-GSH, although not to the same level as the mutant $PfCRT^{Dd2}$ allele. In contrast, we could not demonstrate any [^{3}H]-GSH transport activity in oocytes expressing the CQS allele of *pfcrt*. The only other study in which *pfcrt* has been expressed in oocytes is that reported by Martin and colleagues (26) studying CQ transport. In that study, the *pfcrt* sequence had to be modified extensively to achieve functional expression of the protein in the oocyte system. This was not necessary in the current study where we see adequate and functionally relevant PfCRT protein in the oocyte plasma membrane as well as the oocyte cytoplasm using the unmodified *pfcrt* codon sequence. A further discrepancy between the data presented here for GSH transport and CQ transport reported by Martin and colleagues (26) is that they

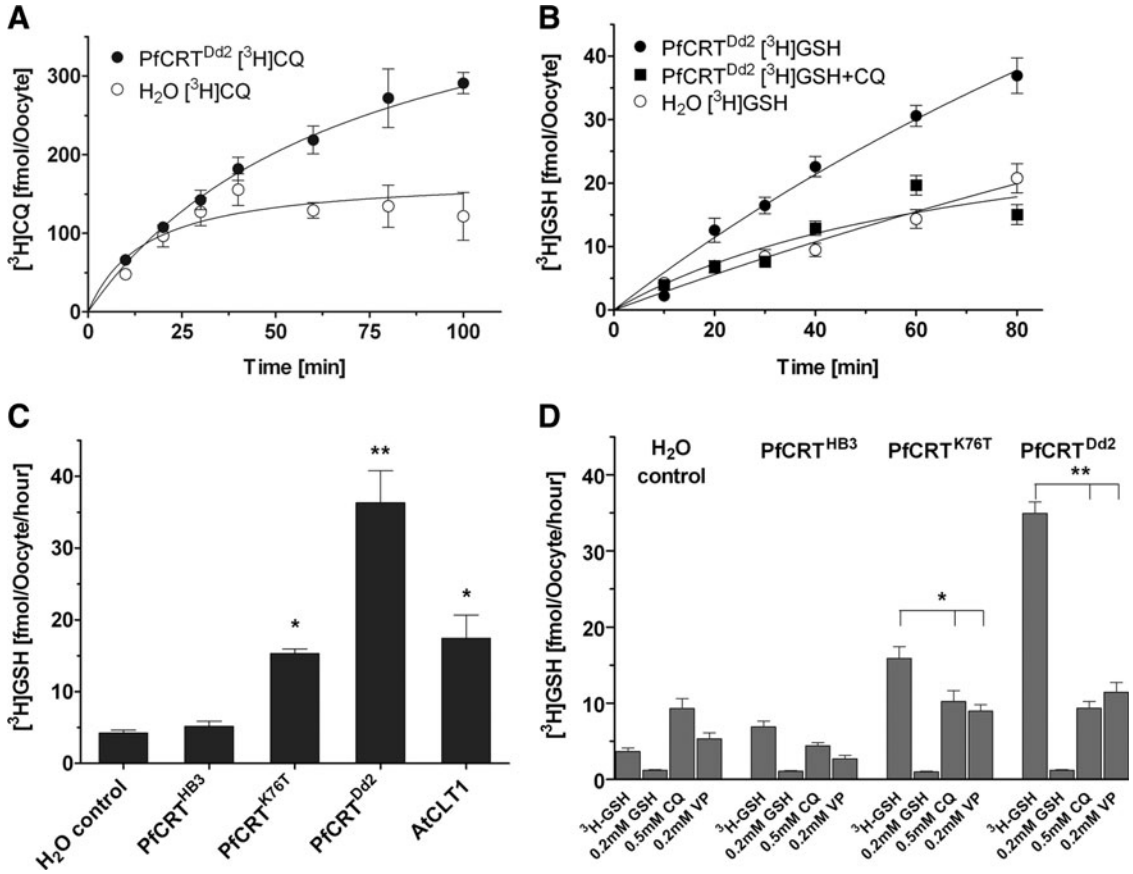

FIG. 6. Uptake of [^{3}H]-GSH by *Xenopus* oocytes expressing mutant and wild-type PfCRT and *Arabidopsis thaliana* CLT1. (A) Time course of uptake of [^{3}H]-CQ in oocytes expressing the mutant PfCRT^{Dd2} (filled circles) in comparison to the water control (open circle). **(B)** Time course of uptake of [^{3}H]-GSH in oocytes expressing PfCRT^{Dd2} in the absence (filled circles) or presence (filled squares) of 0.5 m*M* unlabeled CQ in comparison to the water controls (open circles). Data are means ± S.E.M. from four individual experiments with oocytes from different frogs and with six or more injected oocytes at every time point ($n \geq 24$). GSH accumulation was significantly greater in PfCRT^{Dd2} compared with water-injected controls or PfCRT^{Dd2} in the presence of CQ (*$p < 0.01$, Mann–Whitney *U*-test). **(C)** Uptake of [^{3}H]-GSH in oocytes expressing PfCRT^{HB3}, PfCRT^{K76T}, or PfCRT^{Dd2} variants, together with the positive control from *A. thaliana* (AtCLT1). Data are means ± S.E.M. from five individual experiments with oocytes from different frogs and with seven or more injected oocytes per group (PfCRT isoform or water control) ($n \geq 35$). The PfCRT^{Dd2}-expressing oocytes showed significantly higher uptake of GSH than the water control (**$p < 0.001$, Mann–Whitney *U*-test). A similar trend was observed for PfCRT^{K76T} and AtCLT1 (*$p < 0.01$, Mann–Whitney *U*-test). In contrast, uptake by PfCRT^{HB3} was not significantly different to the water-injected controls. **(D)** Inhibitory effect of unlabeled GSH (0.2 m*M*), CQ (0.5 m*M*), and VP (0.2 m*M*) on the uptake of [^{3}H]-GSH in oocytes expressing PfCRT^{Dd2}, PfCRT^{K76T}, and PfCRT^{HB3}, compared with a water control. Data are means ± S.E.M. from three individual experiments with oocytes from different frogs and with seven or more injected oocytes per group ($n \geq 21$). In the presence of either CQ or VP, the uptake of [^{3}H]-GSH in oocytes expressing PfCRT^{Dd2} was significantly reduced (**$p < 0.001$, Mann–Whitney *U*-test). A similar trend, although less pronounced, was observed for PfCRT^{K76T} (*$p < 0.05$, Mann–Whitney *U*-test). The specificity of the uptake observed in all experimental groups is verified by the reduction of [^{3}H]-GSH uptake to background levels by the coincubation with 0.2 m*M* unlabelled GSH.

found the single-point mutant of PfCRT^{K76T} incapable of CQ transport. Our conclusion is that the K76T mutation in PfCRT generates structural changes that are sufficient to allow GSH transport, but not CQ transport. It is not clear what orientation PfCRT takes when inserted into the oocyte membrane; our results suggest that the majority of the protein has an orientation that is equivalent to that in the DV, or alternatively, the transporter can move GSH in either direction, depending on the prevailing concentration gradient.

Mutant PfCRT has been postulated to act either as a channel, permitting the mediated and fast transport of diprotonated CQ across the DV membrane, or as an outwardly directed slower CQ carrier (6, 26, 35, 39). The transport of GSH is time dependent, but appears to be nonsaturable, which could suggest that the transport is not carrier mediated. Another possibility is that the tripeptide is metabolized by *X. laevis* oocytes, and thus a thermodynamic equilibrium cannot be reached. In either case, the inhibition of GSH transport by CQ and the inhibition of CQ transport by small peptides (26) suggest that CQ and certain peptides, including GSH, share the same translocation sites within mutant PfCRT.

The functional relevance of mutant PfCRT-mediated GSH transport is revealed when GSH levels are elevated in both CQR and CQS parasite lines using NAC, leading to a significant

increase of the CQ IC_{50} values only in CQR lines (Fig. 2). Increased cytoplasmic GSH appears to only access the DV compartment in the CQR parasites, which is consistent with the data presenting GSH transport by mutant PfCRT *in situ*.

Conversely, the GST substrate CDNB is known to reverse CQR, and it was suggested that this was directly caused by a reduction in GSH (14). We show here that incubation of parasites with CDNB as well as reducing intracellular GSH levels also cause CQR parasites to accumulate more CQ (Fig. 3), indicating a clear role for GSH in modulating CQR. However, direct competition between the DNP-SG conjugate and CQ for PfCRT-mediated efflux cannot be completely excluded.

Substitution of mutant *pfcrt* alleles in otherwise isogenic backgrounds of *P. falciparum* has a marked effect on the cellular level of GSH, with CQR isogenic parasites having significantly lower levels of GSH, which is also reflected in their increased susceptibility to BSO (Fig. 2). Our data demonstrate that this is not attributable to changes in the expression of the enzymes involved in the synthesis, conjugation, and reduction of GSH (Fig. 4). Thus, the differences observed in GSH levels are most readily explained as a direct result of the different genotypes of *pfcrt*. We suggest that cytoplasmic GSH is transported into the DV in parasites expressing mutated *pfcrt* and that this is an important feature of CQR.

The CQR parasites contain less GSH than CQS counterparts, which superficially seems strange if this is the mediator of resistance. However, the key factor is not the level of GSH, but its location; it is the GSH in the DV that has the protective effect through binding to heme. This binding itself would reduce the amount of free GSH in the parasite overall, and also there are a multitude of peptidases in the DV, and it seems likely that they eventually destroy much of the DV-located GSH through proteolysis. Proteolysis of GSH and GS-X adducts (which could include GSH–heme) by carboxypeptidases has previously been shown to occur in plant vacuoles, but a fuller investigation of this possibility in *Plasmodium* was beyond the scope of this study (52).

Our findings clearly show that high GSH levels alone are not sufficient to affect CQR; it is the location of the GSH that is central to resistance. This is reiterated by our demonstration that GSH levels in untransformed Dd2 were found to be comparable with those of the CQS lines GC03 and $C2^{GC03}$. This is also supported by a previous study where two nonrelated isolates, CQS 3D7 and CQR Dd2, were compared, and higher GSH levels were reported in the resistant parasites (30). Discovery of the crucial role of the mutant PfCRT in transporting GSH will now allow fuller analyses of the part played by the protein in other CQR lines.

Materials and Methods

Materials

P. falciparum GC03, $C2^{GC03}$, $C3^{Dd2}$, $C6^{7G8}$, T76K-1^{Dd2}, and C-1^{Dd2} were a gift from Professor D. Fidock, (New York, USA) (18, 42) (Table 1). The plasmids *Pf*HSP86 5′-pENTR4/1, GFP-pENTR2/3p, CHD-Hsp86, and pCHD-3/4 were a gift from Professor G. I. McFadden (Melbourne). Anti-*P. falciparum* glutathione *S*-transferase (PfGST) antiserum was obtained from Professor E. Liebau (University of Münster, Germany). Antiserum against *P. falciparum* casein kinase 2α (PfCK2a) was provided by Professor C. Doerig (Monash University, Australia) (16). RPMI 1640 medium and Albumax II were from Invitrogen. All chemicals, unless otherwise stated, were from Sigma.

Parasite culture and determination of IC_{50}s

Parasites were cultured according to Trager and Jensen (46), synchronized using sorbitol (19), and freed from erythrocytes using saponin (47). Parasite drug susceptibility was determined by measuring the incorporation of [^{3}H]-hypoxanthine (20 Ci/mmol; ARC) in the presence of increasing drug concentrations (10) and modifiers of intracellular GSH concentrations as detailed in the figure legends.

Localization studies

Expression constructs pCHD- Hsp86-γGCS-GFP and pCHD- Hsp86-GS-GFP contained the *γgcs* or *gs* genes of *P. falciparum* cloned in frame with a 3′*gfp* gene to generate C-terminal-tagged γ-GCS or GS fusion proteins. The chimeric genes were expressed under the control of the *Pfhsp86* promoter and were generated using the Invitrogen MultiSite Gateway system in combination with the pCHD-3/4 destination vector (48). To generate gene entry clones, the full-length genes for *γgcs* and *gs* were amplified using the primer pairs, defined in Table 2, using *Pfx* SuperMix (Invitrogen) and subcloned according to manufacturer's instructions. The Multisite Gateway LR recombination reaction was performed according to the manufacturer's instructions (Invitrogen).

Determination of total GSH levels

Intracellular GSH levels of saponin-isolated parasites were determined by HPLC (51). Cells were washed once with Earle's balanced salt solution (EBSS) (6.8 g/l NaCl, 0.4 g/l KCl, 0.2 g/l $MgSO_4 \times 7\ H_2O$, 0.158 g/l $NaH_2PO_4 \times 2\ H_2O$, 0.264 g/l $CaCl_2 \times 2\ H_2O$, 2.2 g/l $NaHCO_3$, and 1 g/l D-glucose) before

Table 2. Primers Used in This Study

Product	*Forward primer 5′ to 3′*	*Reverse primer 5′ to 3′*
γgcs ORF	CACCATGGGTTTTCTAAAAATCGGAACG	TGCACTCAGTTCGTACATTTTTTTTGC
gs ORF	CACCATGGAAAGAAAGGTAGATGAGTT	ATGTTCAGTTAAAAAAAAAAGAATCC
Pfcrt cDNA	ATATCTCGAGATGAAATTCGCAAG	ATATCCATGGTTATTGTGTAATAATTGAATCG
γgcs RT-PCR	TCCTTGCTCTTACTGCATGTACT	TTCCGTTCTACAATCAACACTGT
gs RT-PCR	CTTTAGAGCATTATATACACCTAACCA	CGAACCAACAAGTTGATAAGGTA
pfcrt RT-PCR	GGAAATATCCAATCATTTGTTCTT	CAACAATAATAACTGCTCCGAGAT
seryl-tRNA synthase RT-PCR	AAGTAGCAGGTCATCGTGGTT	TTCGGCACATTCTTCCATAA

RT-PCR, real-time quantitative-polymerase chain reaction.

lysis of red blood cells (RBC) with 0.15% saponin (5 min, 4°C). Isolated trophozoites ($2–5 \times 10^7$) were washed 3 times with EBSS, incubated for 45 min at room temperature in 50 μl of 40 m*M* *N*-(2-hydroxyethyl)-piperazine-*N*′(3-propanesulfonic acid) and 4 m*M* diethylenetriamine pentaacetic acid, pH 8.0, with 0.7 m*M* Tris (2-carboxyethyl)-phosphine to fully reduce thiols before derivatisation with monobromobimane. Subsequently, 50 μl of 2 m*M* monobromobimane (dissolved in ethanol) was added, and samples were heated to 70°C for 3 min before extracts were deproteinized for 30 min on ice by addition of 100 μl 4 *M* methane sulfonic acid, pH 1.6. Precipitated protein was removed by centrifugation, and supernatants were subjected to thiol analyses.

CQ uptake and equilibrium binding assays

CQ uptake by *P. falciparum* trophozoites was measured as described previously (5, 18). Steady-state CQ uptake was determined over 20 min using 5 n*M* of [^{3}H]-CQ (specific activity 4.7 Ci/mmol; from ARC) in the presence or absence of various concentrations of CDNB. Equilibrium binding studies were performed as described previously, using 2 n*M* [^{3}H]-CQ and a range of concentrations of unlabelled CQ (18). After correcting for nonspecific uptake (5), the resulting binding isotherms were fitted using nonlinear regression, and binding parameters calculated using the Grafit single-site ligand-binding model (Erithacus).

Determination of parasite hemozoin/heme concentration

P. falciparum-infected RBCs were saponin-lysed, and hemozoin was purified as previously described (18). The protein concentration of parasite lysates was determined using Bradford reagent following the manufacturer's instructions (BioRad). Purified hemozoin was converted into heme by dissolving in 0.5 N NaOH, and heme concentration was determined using a QuantiChrom Heme Assay kit DIHM-250 according to the manufacturer's instructions (Universal Biologicals Ltd). Hemozoin concentration was normalized to mM/mg of protein.

Expression of pfcrt *in* X. laevis *oocytes*

pfcrt cDNA products were synthesized with Thermoscript (Invitrogen) from total RNA of *P. falciparum* and amplified by PCR (primers see Table 2) with Taq High-Fidelity polymerase (Invitrogen) following manufacturer's recommendations. Amplified *pfcrt* (MAL7P1.27) genes from *P. falciparum* HB3 and Dd2 and a third gene only harboring the K76T mutation in the HB3 background constructed using the Quikchange site-directed mutagenesis kit (Stratagene) were directionally cloned into the pSP64T vector (using *Xho*I-*Nco*I sites) for expression in *X. laevis*. The At*clt1* (*Arabidopsis thaliana* chloroquine-like transporter 1; At5g19380) gene (27) was cloned into pT7TS (pGEM4Z-vector; Promega), between *Bgl*II-*Spe*I sites.

Capped complementary RNA (cRNA) was transcribed *in vitro* using the SP6 or T7 Message Machine kits (Ambion) using as templates *Eco*RI-linearized recombinant pSP64T or *Sal*I-linearized pT7TS plasmids, respectively. Oocytes were obtained from *X. laevis* mature females purchased from *Xenopus* Express (Vernassal). *X. laevis* were immersed in euthanasic concentrations (0.5% w/v) of ethyl 3-aminobenzoate methanesulfonate, and 5 m*M* Tris–HCl, pH 7.4. Ovary lobes were removed and divided into smaller sacs. Individual oocytes were isolated manually with a platinum loop (43). After two washes, oocytes were left to recover at 18°C for 2 h in oocyte Ringer's solution (115 m*M* NaCl, 2 m*M* KCl, 1.8 m*M* $CaCl_2$, 1 m*M* $MgSO_4$, 1 m*M* Na_2HPO_4, 1.18 m*M* KH_2PO_4, and 5 m*M* HEPES, pH 7.4; or 5 m*M* MES for pH 6.0; adding 1 ml/l of 10,000 U penicillin/10,000 U streptomycin solution). Stage V–VI oocytes were selected and injected the following day with ~50 ml of DEPC-treated water or cRNA solutions at 1 μg/μl using a semiautomatic injector (Drummond, Nanoject).

GSH uptake assays into X. laevis *oocytes*

Enzymatic defolliculation of oocytes was completed by 30-min incubation in 1 mg/ml collagenase in Ringer's solution (pH 7.4). Radiotracer uptake studies (12 oocytes per condition) were carried out at room temperature in 1 ml Ringer's solution, pH 7.4, with 2 μCi/ml of [^{3}H]-GSH (38.6 Ci/mmol; ARC) and 5% dithiothreitol; the final concentration of GSH was 52 n*M*. [^{3}H]-CQ (4.7 Ci/mmol; ARC) was used at 2 μCi/ml in Ringer's solution, pH 6.0; the final concentration was 425 n*M*. Uptake studies were terminated by washing the oocytes in Ringer's solution, pH 7.4, at 4°C. Individual oocytes were collected and immersed in 1 ml of scintillation liquid. After overnight incubation, radioactivity was determined using a Wallac 1450 Microbeta scintillation counter.

Indirect Immunofluorescence of X. laevis *oocytes expressing PfCRT*

Individual oocytes were immersed in 1 ml of an optimal cutting temperature medium (RA Lamb Ltd), and snap-frozen in 2-methylbutane in liquid N_2 before sections of 10 μm were prepared on glass slides coated with Chrome Alum gelatin solution. Sections were fixed with cold acetone for 10 min, followed by blocking with 4% bovine serum albumin (BSA) in phosphate-buffered saline (PBS) for 1 h, and incubation with primary antibody (1:500 in 4% BSA) for 1 h. After three washes with PBS, secondary anti-rabbit antibody (1:500 in 4% BSA) was applied for 1 h followed by washes as before. Samples were mounted using a VectaShield HardSet mounting medium (Burlingame) and examined by confocal microscopy (Zeiss Axiovert 200 M; L5M5 Pascal laser module).

Isolation of RNA and real-time PCR

RNA was extracted from synchronized trophozoites using Trizol according to the manufacturer's instructions (45). RNA was treated with TURBO-DNA-free before synthesis of cDNA using the RETROscript kit (both Ambion). Real-time quantitative PCR was performed using QuantiTect SYBR Green master mix (Qiagen) and primers at a final concentration of 0.3 μ*M* in a 7500 Real-Time PCR system (Applied Biosystems). Transcription levels of *γgcs*, *gs*, and *pfcrt* were examined using specific primers (Table 2). Seryl-t-RNA synthase was used as an endogenous control (primers see Table 2), as it is transcribed uniformly throughout the parasite life cycle (25, 38). PCR cycling conditions were 50°C for 2 min, 95°C for 15 min, followed by 40 cycles of 95°C for 15 s, 54 for 30 s, and 68°C for 35 s. Relative expression levels were calculated by the ΔΔCT method (User Bulletin 2, Applied Biosystems, www.appliedbiosystems.com).

Western blotting

About 5 μg of protein from four different parasite lines were separated on a 15% SDS-PAGE and blotted onto nitrocellulose. The membrane was probed with the primary antibodies raised against PfGST (1:5000), *P. falciparum* GR (PfGR) (at 1:15,000 dilution), and an antibody raised against PfCK2a (1:200) as a loading control. The secondary anti-rabbit antibody (Promega) was used at 1:10,000 dilution, and the signals were visualized using the Immobilon Western kit (Millipore). Relative expression was analyzed using LabImage 1D software (Kapelan Bio-Imaging Solutions).

Statistical analysis

Statistical analyses were performed using GraphPad Prism 3.0. Parametric data were analyzed by one-way analysis of variance followed by Newman-Keuls post-test if differences were significant. Nonparametric data were analyzed by Mann–Whitney *U*-test. The use of the term significant in the text means a statistically significant difference $p < 0.05$.

Acknowledgments

This work was supported by the Wellcome Trust [WT061173MA-SM]. The research was also supported by the European Community's Seventh Framework Programme [FP7/2007–2013] under grant agreement N° 242095. The Medical Research Council supported PGB and JES-S with the career-developing grant G0400173-69712. The Biotechnology and Biological Sciences Research Council supported SCM and JAHM under the grant BB/C515047/1. The funders had no role in study design, data collection and analysis, decision to publish, or preparation of the manuscript. The authors would like to thank Professors Hagai Ginsburg and Graham H. Coombs for critical reading of the manuscript and many helpful comments.

Ethical Statement

This work involving malaria parasites was carried out using *in vitro* culture of parasites with human RBCs obtained from the West of Scotland Blood Transfusion Service. Ethics approval to use donated blood for this purpose has been obtained from the Scottish National Blood Transfusion Service Review of Nontherapeutic Issues of Blood & Components. All work on genetically modified *Plasmodium falciparum* has been approved by the Health and Safety Executive (GM37/K.09/008, "Genetic manipulation of human malaria parasites for functional genetic analyses"; HSE reference: GM37/02.5). *P. falciparum* wild-type and mutant parasites are contained in Category 3 facilities for all the experimental work and not released into the environment.

Author Disclosure Statement

The authors declare that no competing financial interests exist.

References

1. Atamna H and Ginsburg H. Heme degradation in the presence of glutathione. A proposed mechanism to account for the high levels of non-heme iron found in the membranes of hemoglobinopathic red blood cells. *J Biol Chem* 270: 24876–24883, 1995.
2. Becker K, Rahlfs S, Nickel C, and Schirmer RH. Glutathione—functions and metabolism in the malarial parasite Plasmodium falciparum. *Biol Chem* 384: 551–566, 2003.
3. Bray PG, Hawley SR, Mungthin M, and Ward SA. Physicochemical properties correlated with drug resistance and the reversal of drug resistance in Plasmodium falciparum. *Mol Pharmacol* 50: 1559–1566, 1996.
4. Bray PG, Janneh O, and Ward SA. Chloroquine uptake and activity is determined by binding to ferriprotoporphyrin IX in Plasmodium falciparum. *Novartis Found Symp* 226: 252–260; discussion 260–254, 1999.
5. Bray PG, Mungthin M, Ridley RG, and Ward SA. Access to hematin: the basis of chloroquine resistance. *Mol Pharmacol* 54: 170–179, 1998.
6. Cabrera M, Natarajan J, Paguio MF, Wolf C, Urbach JS, and Roepe PD. Chloroquine transport in Plasmodium falciparum. 1. Influx and efflux kinetics for live trophozoite parasites using a novel fluorescent chloroquine probe. *Biochemistry* 48: 9471–9481, 2009.
7. Cabrera M, Paguio MF, Xie C, and Roepe PD. Reduced digestive vacuolar accumulation of chloroquine is not linked to resistance to chloroquine toxicity. *Biochemistry* 48: 11152–11154, 2009.
8. Chou AC and Fitch CD. Hemolysis of mouse erythrocytes by ferriprotoporphyrin IX and chloroquine. Chemotherapeutic implications. *J Clin Invest* 66: 856–858, 1980.
9. Chou AC, Chevli R, and Fitch CD. Ferriprotoporphyrin IX fulfills the criteria for identification as the chloroquine receptor of malaria parasites. *Biochemistry* 19: 1543–1549, 1980.
10. Desjardins RE, Canfield CJ, Haynes JD, and Chulay JD. Quantitative assessment of antimalarial activity *in vitro* by a semiautomated microdilution technique. *Antimicrob Agents Chemother* 16: 710–718, 1979.
11. Fidock DA, Nomura T, Talley AK, Cooper RA, Dzekunov SM, Ferdig MT, Ursos LM, Sidhu AB, Naude B, Deitsch KW, Su XZ, Wootton JC, Roepe PD, and Wellems TE. Mutations in the P. falciparum digestive vacuole transmembrane protein PfCRT and evidence for their role in chloroquine resistance. *Mol Cell* 6: 861–871, 2000.
12. Foote SJ, Thompson JK, Cowman AF, and Kemp DJ. Amplification of the multidrug resistance gene in some chloroquine-resistant isolates of P. falciparum. *Cell* 57: 921–930, 1989.
13. Ginsburg H and Golenser J. Glutathione is involved in the antimalarial action of chloroquine and its modulation affects drug sensitivity of human and murine species of Plasmodium. *Redox Rep* 8: 276–279, 2003.
14. Ginsburg H, Famin O, Zhang J, and Krugliak M. Inhibition of glutathione-dependent degradation of heme by chloroquine and amodiaquine as a possible basis for their antimalarial mode of action. *Biochem Pharmacol* 56: 1305–1313, 1998.
15. Gligorijevic B, Purdy K, Elliott DA, Cooper RA, and Roepe PD. Stage independent chloroquine resistance and chloroquine toxicity revealed via spinning disk confocal microscopy. *Mol Biochem Parasitol* 159: 7–23, 2008.
16. Holland Z, Prudent R, Reiser JB, Cochet C, and Doerig C. Functional analysis of protein kinase CK2 of the human malaria parasite Plasmodium falciparum. *Eukaryot Cell* 8: 388–397, 2009.
17. Johnson DJ, Fidock DA, Mungthin M, Lakshmanan V, Sidhu AB, Bray PG, and Ward SA. Evidence for a central role for PfCRT in conferring Plasmodium falciparum resistance to diverse antimalarial agents. *Mol Cell* 15: 867–877, 2004.
18. Lakshmanan V, Bray PG, Verdier-Pinard D, Johnson DJ, Horrocks P, Muhle RA, Alakpa GE, Hughes RH, Ward SA,

Krogstad DJ, Sidhu AB, and Fidock DA. A critical role for PfCRT K76T in Plasmodium falciparum verapamil-reversible chloroquine resistance. *Embo J* 24: 2294–2305, 2005.
19. Lambros C and Vanderberg JP. Synchronization of Plasmodium falciparum erythrocytic stages in culture. *J Parasitol* 65: 418–420, 1979.
20. Leed A, DuBay K, Ursos LM, Sears D, De Dios AC, and Roepe PD. Solution structures of antimalarial drug-heme complexes. *Biochemistry* 41: 10245–10255, 2002.
21. Li L, Lee TK, and Ballatori N. Functional re-evaluation of the putative glutathione transporters, RcGshT and RsGshT. *Yale J Biol Med* 70: 301–310, 1997.
22. Liebau E, Bergmann B, Campbell AM, Teesdale-Spittle P, Brophy PM, Luersen K, and Walter RD. The glutathione S-transferase from Plasmodium falciparum. *Mol Biochem Parasitol* 124: 85–90, 2002.
23. Lüersen K, Walter RD, and Müller S. Plasmodium falciparum-infected red blood cells depend on a functional glutathione *de novo* synthesis attributable to an enhanced loss of glutathione. *Biochem J* 346 Pt 2: 545–552, 2000.
24. Lüersen K, Walter RD, and Müller S. The putative gamma-glutamylcysteine synthetase from Plasmodium falciparum contains large insertions and a variable tandem repeat. *Mol Biochem Parasitol* 98: 131–142, 1999.
25. Mamoun CB and Goldberg DE. Plasmodium protein phosphatase 2C dephosphorylates translation elongation factor 1beta and inhibits its PKC-mediated nucleotide exchange activity *in vitro*. *Mol Microbiol* 39: 973–981, 2001.
26. Martin RE, Marchetti RV, Cowan AI, Howitt SM, Broer S, and Kirk K. Chloroquine transport via the malaria parasite's chloroquine resistance transporter. *Science* 325: 1680–1682, 2009.
27. Maughan SC, Pasternak M, Cairns N, Kiddle G, Brach T, Jarvis R, Haas F, Nieuwland J, Lim B, Muller C, Salcedo-Sora E, Kruse C, Orsel M, Hell R, Miller AJ, Bray P, Foyer CH, Murray JA, Meyer AJ, and Cobbett CS. Plant homologs of the Plasmodium falciparum chloroquine-resistance transporter, PfCRT, are required for glutathione homeostasis and stress responses. *Proc Natl Acad Sci U S A* 107: 2331–2336, 2010.
28. McIlwain CC, Townsend DM, and Tew KD. Glutathione S-transferase polymorphisms: cancer incidence and therapy. *Oncogene* 25: 1639–1648, 2006.
29. Meierjohann S, Walter RD, and Müller S. Glutathione synthetase from Plasmodium falciparum. *Biochem J* 363: 833–838, 2002.
30. Meierjohann S, Walter RD, and Müller S. Regulation of intracellular glutathione levels in erythrocytes infected with chloroquine-sensitive and chloroquine-resistant Plasmodium falciparum. *Biochem J* 368: 761–768, 2002.
31. Meister A. Glutathione metabolism and its selective modification. *J Biol Chem* 263: 17205–17208, 1988.
32. Mu J, Ferdig MT, Feng X, Joy DA, Duan J, Furuya T, Subramanian G, Aravind L, Cooper RA, Wootton JC, Xiong M, and Su XZ. Multiple transporters associated with malaria parasite responses to chloroquine and quinine. *Mol Microbiol* 49: 977–989, 2003.
33. Naude B, Brzostowski JA, Kimmel AR, and Wellems TE. Dictyostelium discoideum expresses a malaria chloroquine resistance mechanism upon transfection with mutant, but not wild-type, Plasmodium falciparum transporter PfCRT. *J Biol Chem* 280: 25596–25603, 2005.
34. Pagola S, Stephens PW, Bohle DS, Kosar AD, and Madsen SK. The structure of malaria pigment beta-haematin. *Nature* 404: 307–310, 2000.
35. Paguio MF, Cabrera M, and Roepe PD. Chloroquine transport in Plasmodium falciparum. 2. Analysis of PfCRT-mediated drug transport using proteoliposomes and a fluorescent chloroquine probe. *Biochemistry* 48: 9482–9491, 2009.
36. Raj DK, Mu J, Jiang H, Kabat J, Singh S, Sullivan M, Fay MP, McCutchan TF, and Su XZ. Disruption of a Plasmodium falciparum multidrug resistance-associated protein (PfMRP) alters its fitness and transport of antimalarial drugs and glutathione. *J Biol Chem* 284: 7687–7696, 2009.
37. Reed MB, Saliba KJ, Caruana SR, Kirk K, and Cowman AF. Pgh1 modulates sensitivity and resistance to multiple antimalarials in Plasmodium falciparum. *Nature* 403: 906–909, 2000.
38. Salanti A, Staalsoe T, Lavstsen T, Jensen AT, Sowa MP, Arnot DE, Hviid L, and Theander TG. Selective upregulation of a single distinctly structured var gene in chondroitin sulphate A-adhering Plasmodium falciparum involved in pregnancy-associated malaria. *Mol Microbiol* 49: 179–191, 2003.
39. Sanchez CP, Stein WD, and Lanzer M. Is PfCRT a channel or a carrier? Two competing models explaining chloroquine resistance in Plasmodium falciparum. *Trends Parasitol* 23: 332–339, 2007.
40. Sanchez CP, Wunsch S, and Lanzer M. Identification of a chloroquine importer in Plasmodium falciparum. Differences in import kinetics are genetically linked with the chloroquine-resistant phenotype. *J Biol Chem* 272: 2652–2658, 1997.
41. Shviro Y and Shaklai N. Glutathione as a scavenger of free hemin. A mechanism of preventing red cell membrane damage. *Biochem Pharmacol* 36: 3801–3807, 1987.
42. Sidhu AB, Verdier-Pinard D, and Fidock DA. Chloroquine resistance in Plasmodium falciparum malaria parasites conferred by pfcrt mutations. *Science* 298: 210–213, 2002.
43. Sigel E and Minier F. The Xenopus oocyte: system for the study of functional expression and modulation of proteins. *Mol Nutr Food Res* 49: 228–234, 2005.
44. Slater AF and Cerami A. Inhibition by chloroquine of a novel haem polymerase enzyme activity in malaria trophozoites. *Nature* 355: 167–169, 1992.
45. Smith JD, Kyes S, Craig AG, Fagan T, Hudson-Taylor D, Miller LH, Baruch DI, and Newbold CI. Analysis of adhesive domains from the A4VAR Plasmodium falciparum erythrocyte membrane protein-1 identifies a CD36 binding domain. *Mol Biochem Parasitol* 97: 133–148, 1998.
46. Trager W and Jensen JB. Human malaria parasites in continuous culture. *Science* 193: 673–675, 1976.
47. Umlas J and Fallon JN. New thick-film technique for malaria diagnosis. Use of saponin stromatolytic solution for lysis. *Am J Trop Med Hyg* 20: 527–529, 1971.
48. van Dooren GG, Marti M, Tonkin CJ, Stimmler LM, Cowman AF, and McFadden GI. Development of the endoplasmic reticulum, mitochondrion and apicoplast during the asexual life cycle of Plasmodium falciparum. *Mol Microbiol* 57: 405–419, 2005.
49. Waller KL, Muhle RA, Ursos LM, Horrocks P, Verdier-Pinard D, Sidhu AB, Fujioka H, Roepe PD, and Fidock DA. Chloroquine resistance modulated *in vitro* by expression levels of the Plasmodium falciparum chloroquine resistance transporter. *J Biol Chem* 278: 33593–33601, 2003.
50. Warhurst DC. The quinine-haemin interaction and its relationship to antimalarial activity. *Biochem Pharmacol* 30: 3323–3327, 1981.
51. Williams RA, Westrop GD, and Coombs GH. Two pathways for cysteine biosynthesis in Leishmania major. *Biochem J* 420: 451–462, 2009.

52. Wolf AE, Dietz KJ, and Schroder P. Degradation of glutathione S-conjugates by a carboxypeptidase in the plant vacuole. *FEBS Lett* 384: 31–34, 1996.

Address correspondence to:
Prof. Sylke Müller
Institute of Infection
Immunity and Inflammation
College of Medical
Veterinary and Life Sciences
University of Glasgow
120 University Place
Glasgow G12 8TA
United Kingdom

E-mail: sylke.muller@glasgow.ac.uk

Prof. Stephen A. Ward
Molecular and Biochemical Parasitology Group
Liverpool School of Tropical Medicine
Pembroke Place
Liverpool L3 5QA
United Kingdom

E-mail: saward@liverpool.ac.uk

Date of first submission to ARS Central, March 28, 2012; date of final revised submission, October 26, 2012; date of acceptance, November 11, 2012.

Abbreviations Used

ANOVA = analysis of variance
AtCLT = PfCRT-like proteins from *Arabidopsis thaliana*
BSA = bovine serum albumin
BSO = L-buthionine sulfoximine
CAR = cellular accumulation ratio for chloroquine
CDNB = 1-chloro-2,4-dinitrobenzene
CQ = chloroquine
CQR = CQ-resistant and CQ resistance
CQS = CQ sensitive
DV = digestive vacuole
EBSS = Earle's balanced salt solution
GFP = green fluorescent protein
GSH = glutathione
GST = glutathione *S*-transferase
NAC = *N*-acetylcysteine
PBS = phosphate-buffered saline
PCR = polymerase chain reaction
PfCK2a = *P. falciparum* casein kinase 2α
PfCRT = *Plasmodium falciparum* chloroquine resistance transporter
PfGR = *P. falciparum* glutathione reductase
PfGS = *P. falciparum* glutathione synthetase
PfγGCS = *P. falciparum* γ-glutamylcysteine synthetase
RBC = red blood cells
RT-PCR = real time quantitative polymerase chain reaction
VP = verapamil